

Analytical Ultracentrifugation for Characterizing Nanocrystals and Their Bioconjugates

Michelle Calabretta,[†] Jennifer A. Jamison,[‡] Joshua C. Falkner,[‡] Yunping Liu,[‡] Benjamin D. Yuhas,[‡] Kathleen S. Matthews,[†] and Vicki L. Colvin^{*‡}

The Department of Biochemistry and Cell Biology and The Department of Chemistry, Rice University, Houston, Texas 77005

Received December 14, 2004

ABSTRACT

Analytical ultracentrifugation (AU) provides a general way to probe the polydispersity of nanoparticles and the formation of bioconjugates in solution. Unconjugated gold nanocrystals show sedimentation coefficient distributions that are in agreement with size distributions as measured by TEM. AU is sensitive to the size/shape changes elicited by conjugation, in this case to lactose repressor (Lacl). AU data reveal saturating protein concentrations for conjugates that correspond to the measured stoichiometry of the complex under these conditions.

Introduction. Applying the unique features of nanoscale structures in biological applications generally requires the formation of nanoparticle/biomolecule conjugates, where a nanoscale particle is tethered through chemical or physical means to an active biomolecule. Historically, gold nanocrystal/antibody conjugates have found widespread use in biological research as labels for electron microscopy.¹ More recently, nanoscale structures have been conjugated to various biomolecules for DNA detection assays,^{2–5} biological labeling,^{6–9} immunoassays,^{10–12} and materials assembly.^{13–16} In all of these settings, physical characterization of conjugates is central for their optimization in applications. Tools that can provide information about the formation of conjugates and the stoichiometry of their components are thus essential to generating more effective nanobiological systems.

The general problem of nano/bio conjugate characterization is challenging, as this requires not only evaluation of disparate components of a hybrid material, but also the properties of the entire assembly. Traditional biotechnology and nanotechnology techniques are difficult to adapt directly for this purpose. For example, ultraviolet absorbance is frequently used to determine protein concentration in solution, but optical signatures of nanocrystals (e.g., gold, CdSe) interfere with this routine, quantitative analysis for conjugated proteins. Optical spectroscopy can be useful in specific circumstances, however. Single-stranded DNA-gold nanocrystal conjugate systems, for instance, change color from

red to blue as DNA hybridization induces cross-linking between nanocrystals.^{2,17} Alternatively, transmission electron microscopy (TEM) is widely used for evaluating nanocrystal shape and quality but is not well suited for visualizing the biomolecular coating on nano/bio conjugates. Nonetheless, in some instances, average interparticle spacings from dried nano/bio conjugate films have been used to evaluate conjugation effectiveness.^{15,16,18} More recently, the stoichiometry, structure, and conformations of DNA-gold nanocrystal conjugates have been evaluated with electrophoresis.^{19–21} Similarly, electrophoresis has also been applied to protein–nanocrystal conjugates, but stoichiometric and structural analysis of conjugates is impeded by the strong charge characteristics of nanostructures.^{11,22} Further, this method is not readily applicable to very large complexes, sample recovery is challenging, and application to nonaqueous particle systems is not feasible. Analytical ultracentrifugation (AU) is an ideal complement to these existing modes of analysis. This solution technique can be applied to both aqueous and nonaqueous systems, with detection at any wavelength across the UV–visible spectrum. Moreover, AU allows recovery of the analyzed sample.

Ultracentrifugation is routinely used as a separation tool for biological macromolecules. When performed analytically, this method provides detailed quantitative information about the mass and shape of proteins and their complexes in solution.²³ In nanoscience, centrifugation has been applied as a preparative technique through the common process of size selective centrifugation.²⁴ Furthermore, coarse centrifugation has also been used to separate free biomolecules from conjugates, thereby facilitating quantitative calculations on

* Corresponding author. Telephone 713-348-5741; Fax 713-348-5155; E-mail: colvin@rice.edu.

[†] The Department of Biochemistry and Cell Biology.

[‡] The Department of Chemistry.

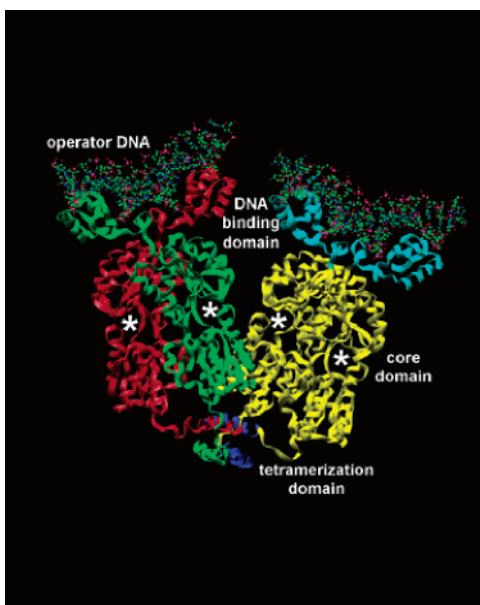


Figure 1. Crystallographic structure of homotetrameric LacI bound to operator DNA. The LacI dimer is the DNA binding unit. In the right dimer, the DNA binding domain is shown in light blue, the core domain in yellow, and the tetramerization domain in dark blue. The sugar-binding pocket is indicated by the asterisk in each subunit. The left dimer shows the two monomers in red and green. The structure was generated from the PDB file 1lbg as reported by Lewis et al.⁴³

conjugate activity.^{25,26} Recently, analytical centrifugation has been applied to nonbiologically bound nanoscale structures to determine particle size distribution and detect changes in surface structure.^{27–30} We demonstrate here that analytical applications of ultracentrifugation can provide physical information about nanostructures and their bioconjugates directly and nondestructively in the solution phase.

For this work, we evaluated the systematic changes in the sedimentation properties of gold nanocrystals conjugated to the oligomeric DNA binding protein LacI (Figure 1). DNA recognition proteins have been the subject of interest in nanoscience: for example, where fluorescent particle protein conjugates are assessed for specific DNA recognition,³¹ where particles are bound to DNA first,^{32,33} or where DNA-protein complexes are used as scaffolds for fabrication of gold nanostructures.³⁴ LacI is a particularly attractive substrate for conjugation because of the extensive genetic, biochemical, and biophysical information available for this protein.³⁵ Although a level of complexity is introduced using LacI as a bioconjugate, the benefits of that complexity emerge in the possible applications. LacI binds two ligands, DNA and sugar, and the protein exhibits allosteric binding behavior (i.e., the binding of one ligand affects affinity for the other ligand).³⁵ Thus, LacI conjugates have the potential to provide control over conjugate function because bound DNA can be released by the addition of sugar. Here we show that analytical ultracentrifugation can detect the changes in sedimentation that result when LacI is conjugated to gold nanoparticles. This information can be used to determine the extent of the conjugation process as well as an average

stoichiometry (i.e., number of proteins/nanoparticle) of nano/bio conjugates.

Methods. For this work, gold nanocrystals of diameter ~ 10 nm were purchased from Ted Pella (Sample A). Additionally, gold nanocrystals were prepared according to the methods detailed by Frens et al. (Sample B).³⁶ Typically 38.8 mM sodium citrate (Aldrich, 99%) was added to 50 mL of boiling 1 mM $\text{HAuCl}_4 \cdot 3\text{H}_2\text{O}$ (Aldrich, A.C.S.). The color of the mixture changed from yellow to colorless to deep red, indicating the formation of gold nanocrystals. We estimate gold nanocrystal concentrations in water, from both TEM as well as the reaction yields, as 14 nM for our solutions. TEM grids were prepared by evaporating approximately 20 μL of gold nanocrystal solution onto a Ted Pella 300 mesh grid with removable Formvar and a 5–10 nm thick amorphous carbon film. Samples were imaged in a JEOL-2010 transmission electron microscope operating at 100 kV; approximately 5 images were digitally recorded at 40 000 \times magnification. ImagePro software was used to count approximately 500 nanocrystals for each sample to produce the average size and size distribution of the gold core. Gold nanocrystals in this work have an average diameter of 10.1 ± 1.1 nm (Sample A) and 13.8 ± 3.0 nm (Sample B).

Purification of LacI was carried out as described previously.³⁷ Proteins were expressed in *E. coli* strain BLIM (a derivative of BL26 cured of the LacI episome).³⁸ Following centrifugation of cultures, cell pellets were resuspended and lysed. Cell lysis supernatant was precipitated with 37% ammonium sulfate, dialyzed, and loaded onto a phosphocellulose column. The protein was eluted with a gradient of 0.12–0.3 M potassium phosphate buffer. Fractions containing LacI, as determined by SDS–PAGE, were collected, and concentrations were determined by absorbance at 280 nm ($\epsilon = 0.6 \text{ cm}^{-1} \text{ mg}^{-1} \text{ mL}$). [³⁵S]-Methionine labeled LacI was generated with the TNT T7 Quick for PCR DNA transcription/translation kit (Promega) using the provided protocol. Briefly, the LacI gene was cloned into the pGEM-T vector (Promega) under the T7 promoter. After translation in the presence of [³⁵S]-methionine (ICON Isotopes), unincorporated radioactivity was removed from labeled protein with protein desalting spin columns (Pierce). [³⁵S]-LacI was further purified from reaction components on a small phosphocellulose column. Purified [³⁵S]-LacI was diluted 1:1 with unlabeled LacI before protein concentration was determined by the absorbance at 280 nm. The amount of radiolabel (counts per minute or cpm) was measured for an aliquot of this mixture to arrive at a specific activity (cpm/ μg) for the sample.

Conjugates were formed as follows: LacI was dialyzed against 50 mM Tris, pH 10, 5% glucose, 0.1 mM dithiothreitol (conjugation buffer) in order to remove the potassium phosphate from the storage buffer. Gold nanocrystals (250 μL) were diluted 1:1 with conjugation buffer, mixed with dialyzed LacI to specified concentrations, and then diluted to 1 mL with conjugation buffer (final concentration of gold nanocrystal ~ 3.5 nM). Samples were allowed to conjugate for 30 min at room temperature. Under these conditions, nanocrystals were stable against aggregation and exhibited

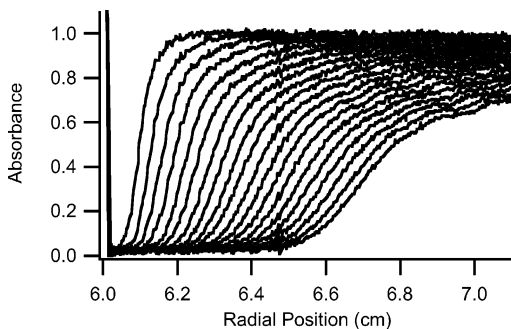


Figure 2. Example sedimentation velocity raw data for Sample A ($D=10.1 \pm 1.1$ nm). Nanocrystals were centrifuged at an angular velocity of 4000 rpm. Absorbance scans were taken at 520 nm throughout the cell length every 6 min. The first scan is the left-most, and the last scan is the right-most. The radial position shown on the x -axis is the distance from the center of the rotor.

a red color for weeks. For [35 S]-LacI conjugates, free protein was first removed by centrifugation and resuspension of the pellet. The concentration of the conjugated protein was determined based on the amount of radiolabel present in the sample. This analysis provided a quantitative measure of protein concentration conjugated to nanoparticles through the specific activity of the initial protein sample. The average concentration of LacI was 24 ± 2.8 nM ($n = 3$) when conjugated to 3.5 nM Sample B, corresponding to a LacI to gold nanocrystal ratio of approximately 7:1 for Sample B.

Analytical ultracentrifugation data were collected on a Beckman XL-A analytical ultracentrifuge using the vendor's software. The quartz cell windows were cleaned with aqua regia after each experiment to remove attached gold material and thus prevent cell leakage and optical interference. Sedimentation velocity experiments were performed at 20 °C at specified angular velocities. Scans were taken every 6 min for up to 120 scans, and data were processed with Ultrascan version 6.2.³⁹ In all data sets, 80% or more of the boundary was used for fitting by the enhanced van Holde-Weischet analysis in Ultrascan.

Results. Biologists have developed analytical ultracentrifugation as a powerful tool for evaluating the hydrodynamic properties, molecular weight, and shape of biomolecules. In a typical sedimentation velocity experiment, raw data are displayed as absorbance traces obtained from time-dependent changes in solution absorbance as a function of radial position. To illustrate, example data are shown in Figure 2. As time proceeds, particles sediment with the centrifugal force, causing a boundary of optical density to move outward from the center of the rotor. This resulting family of curves can be quantitated to deduce the number and relative frequency of sedimenting species and their corresponding sedimentation coefficients, or S -values. The S -value, with dimensions 10^{-13} seconds, is derived from the sedimentation velocity of the molecule in a centrifugal field. This value is dependent not only on particle molecular weight, shape, and density, but also viscosity and density of the solvent. The S -value thus captures details of the material's physical properties. The van Holde-Weischet method of data analysis is particularly well suited for conjugate characterization because it is sensitive to heterogeneity in samples of

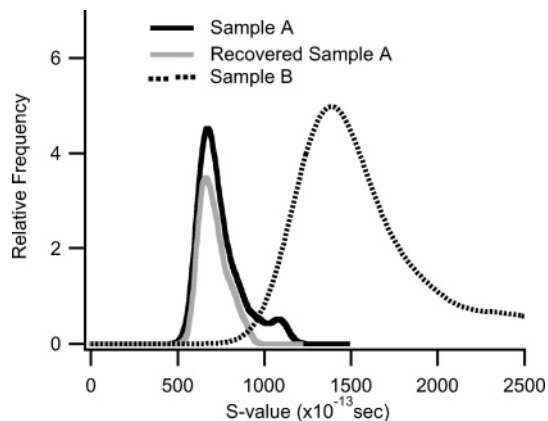


Figure 3. S -values derived for Sample A ($D = 10.1 \pm 1.1$ nm) and Sample B ($D = 13.8 \pm 3.0$ nm). The relative frequency of different S -values is plotted. Sample A (black line) and a recovered sample rerun in the AU under the same conditions (gray line). The samples show a broad (>500) S -value distribution. Larger S -value species, presumably aggregated material, cannot be resuspended in the recovered sample and therefore disappear from the analyzed data. The prepared nanocrystals in Sample B (broken line) have a larger diameter and therefore a larger S -value than the purchased nanocrystals in Sample A. They also show greater polydispersity as compared to Sample A, in good agreement with TEM data (see Supporting Information).

unknown composition, and its assumptions have been shown to be valid for a range of biomolecular problems. Readers are directed elsewhere for detailed discussion of van Holde-Weischet analysis.^{40,41} Here, we have applied AU and van Holde-Weischet analysis (1) to assess the polydispersity of commercial and prepared gold nanocrystals, (2) to measure the effect of protein conjugation on the sedimentation properties of gold nanocrystals, and (3) to evaluate the efficiency and stoichiometry of conjugation.

To establish the utility of AU, we calculated theoretical sedimentation coefficients for two different sizes of gold nanocrystals from different sources and compared the results to measured S -values. The theoretical sedimentation coefficient, S , for a smooth, compact, and spherical particle is given by eq 1:

$$S = \frac{MW(1 - \bar{v}\rho_s)}{A6\pi\eta_s r f} \quad (1)$$

where MW is molecular weight, \bar{v} is the partial specific volume of the particle, ρ_s is the density of the solvent, A is Avogadro's number, η_s is the viscosity of the solvent, r is the radius of the particle, and f is the frictional coefficient ($f = 1$ for a sphere). In the case of a nonspherical particle, the frictional coefficient can alter the S -value substantially. Assuming a spherical particle, a gold nanocrystal density of 17 g/cm^3 in eq 1,⁴² and using the diameter and polydispersity as determined from TEM, we calculated theoretical S -value ranges for Sample A (650–1010 S) and Sample B (940–2260), respectively. The nanocrystals were then analyzed with AU. Figure 3 shows S -value distributions calculated from van Holde-Weischet analysis of the resulting AU data from Samples A and B. The smaller nanocrystals in Sample

A (Figure 3, black line) show a sedimentation coefficient range between 500 and 1200 S, with a peak at approximately 670 S. The measured and theoretical S-values are therefore in good agreement, considering the severity of the assumptions made for the theoretical calculations.

An important advantage of AU in nanocrystal analysis is that it is a nondestructive method; samples can be recovered after sedimentation, permitting further analysis or purification. The dashed line in Figure 3 illustrates this feature directly. After sedimentation, Sample A was recovered, resuspended, and rerun in the AU under the same conditions. The S-value of the recovered sample (gray line, Figure 3) is comparable to the initial sample, having a maximum of 660 S. The most significant change is the decrease in the amount of larger species (or aggregates) at higher S-values, presumably due to difficulty in their resuspension after the initial sedimentation. These data illustrate that the integrity of the sample is not disrupted by sedimentation, and samples can thus be recovered for further use and analysis.

Compared to Sample A, the larger gold nanocrystals in Sample B (Figure 3, broken line) have a broader and higher S-value range, 1000–2500 S, with a peak at 1380 S. This breadth is expected given the larger 3.0 nm standard deviation in size for Sample B. As for Sample A, we find that theoretical S-values are in reasonably good agreement with the experimentally obtained S-values. In effect, these sedimentation data capture the polydispersity of gold nanocrystals and accurately reflect the distribution of sizes seen from TEM data (see Supporting Information).

When Sample B is conjugated to LacI and analyzed with AU, large and systematic changes in sedimentation behavior are observed. The gray line in Figure 4A depicts the S-value histogram for the conjugate. Compared to the unconjugated nanocrystals (Figure 4A, black line), the maximum has shifted to 860 S, about a 500 S-value decrease. Even though the conjugate has a larger theoretical molecular weight than free nanocrystal, the S-value decrease arises from the combined effects of a substantially decreased density (inversely related to partial specific volume) and an increased frictional coefficient (see eq 1). The observed conjugate S-value is also significantly higher than that of free protein (~7 S for LacI, not shown). As with unconjugated nanocrystals, conjugates recovered and rerun have very similar S-value distributions to the initial run. In summary, AU is able to detect the formation of protein nanocrystal conjugates while maintaining the integrity of the sample.

LacI saturation of nanocrystals in Sample B can be followed with AU as demonstrated in Figure 4B. As more protein is added to the nanocrystals, the S-values reach a minimum at which no further decrease in S-value is observed. These data show that AU can provide a quantitative measure of the extent of conjugation without prior separation of free and conjugated protein. The protein concentration corresponding to the minimum S-value “end point”, approximately 25 nM, is similar to the concentration of conjugated LacI (24.4 nM) as determined by the specific activity of [³⁵S]-LacI (see Methods). The value calculated from AU corresponds to a LacI tetramer to gold nanocrystal ratio of 7:1.

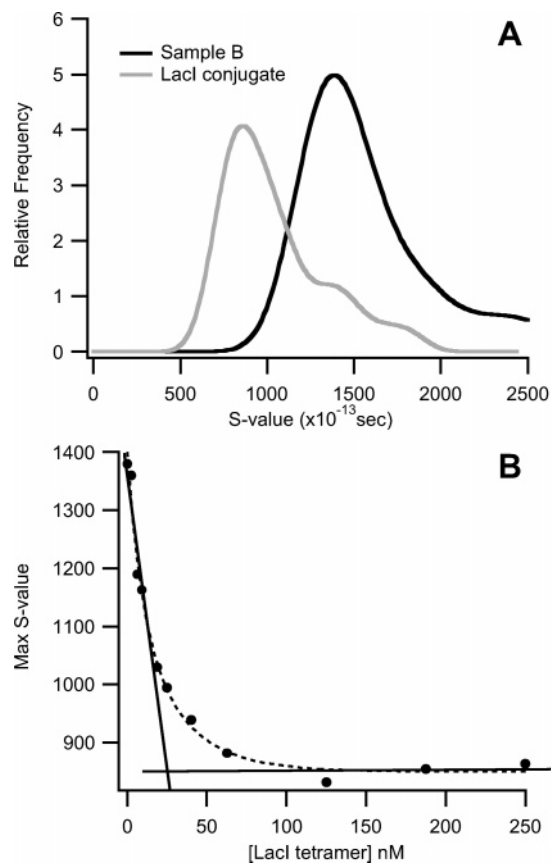


Figure 4. Effect of protein conjugation on the sedimentation of Sample B ($D = 13.8 \pm 3.0$ nm). Sample B conjugated to a range of LacI concentrations (6.25 to 250 nM) was centrifuged at an angular velocity of 3100 rpm. (A) Comparison of S-values for Sample B (black line) and its conjugate to 250 nM LacI (gray line). Free LacI is approximately 7 S and is not shown. (B) Effect of increasing protein concentration on conjugate peak S-values. The maximum peak S-values obtained are plotted against the protein concentration. Increased protein concentrations result in a sequential shift of the S-value peaks. Eventually, the nanocrystals become saturated at approximately 25 nM LacI, in good agreement with the concentration of conjugated LacI (24 nM) as determined by the amount of [³⁵S]-LacI bound.

(Stoichiometry can be measured only if the protein·particle K_d is well below the concentrations required for the experiment. Additional experiments done at varied component concentrations show that this requirement is met for our protein·particle system.) Additionally, calculations approximating the contact surface area of LacI from its crystal structure⁴³ show that approximately 6 LacI tetramers per gold nanocrystal would be accommodated on a nanocrystal with an average diameter of 13.8 nm. Although these two values are in reasonably good agreement, the measured ratio is larger than expected for a variety of reasons: Proteins are more flexible in the solution phase as opposed to in a crystal structure, which may allow for more efficient packing onto the nanocrystal surface. Further, the difference may arise from the mathematical observation that the average surface area in a population is larger than that computed using an average diameter.⁴² Despite these challenges, this example illustrates that AU can provide a quantitative measure of the

extent of conjugation, resulting in the stoichiometry of a fully conjugated nanocrystal.

Discussion. The results presented illustrate the utility of analytical ultracentrifugation as a solution phase technique for evaluating the size, dispersity, and protein conjugation of nanoparticle systems. The gold nanocrystal solutions examined exhibit a broad distribution in the measured sedimentation coefficients that corresponds to the size distribution observed by TEM (see Supporting Information). AU analysis does not disrupt the integrity of the nanocrystals or their protein conjugates, and the samples can be recovered for further use. Further, the technique is broadly applicable to any type of particle in solution, regardless of particle composition or solvent. Most importantly, analytical ultracentrifugation is sensitive to conjugate formation, thereby distinguishing between conjugated and free nanocrystal due to changes in complex size, density, and hydrodynamic properties. Finally, when the concentrations of conjugate components are varied, AU is capable of measuring conjugation efficiency and the average stoichiometry of a fully conjugated nanocrystal without prior removal of free protein. In the future, other parameters affecting conjugation can be analyzed with this technique in order to optimize the process and develop functional materials.

Acknowledgment. We thank Dr. Borries Demeler and Dr. Susan Cates for their help with data analysis. This work is supported in part by the Nanoscale Science and Engineering Initiative of the National Science Foundation under NSF Award Number EEC-0118007, The National Institutes of Health (GM22441), and the Robert A Welch Foundation (C-576).

Supporting Information Available: TEM data of particle samples and diameter frequency histograms of particle samples from TEM data. This material is available free of charge via the Internet at <http://pubs.acs.org>.

References

- (1) Handley, D. A. In *Colloidal Gold: Principles, Methods and Applications*; Hayat, M. A., Ed.; Academic Press: San Diego, CA, 1989; Vol. 1, pp 1–12.
- (2) Storhoff, J. J.; Elghanian, R.; Mucic, R. C.; Mirkin, C. A.; Letsinger, R. L. *J. Am. Chem. Soc.* **1998**, *120*, 1959–1964.
- (3) He, L.; Musick, M. D.; Nicewarner, S. R.; Salinas, F. G.; Benkovic, S. J.; Natan, M. J.; Keating, C. D. *J. Am. Chem. Soc.* **2000**, *122*, 9071–9077.
- (4) Taton, T. A.; Mirkin, C. A.; Letsinger, R. L. *Science* **2000**, *289*, 1757–1760.
- (5) Park, S.-J.; Taton, T. A.; Mirkin, C. A. *Science* **2002**, *295*, 1503–1506.
- (6) Bruchez, M.; Moronne, M.; Gin, P.; Weiss, S.; Alivisatos, A. P. *Science* **1998**, *281*, 2013–2016.
- (7) Chan, W. C. W.; Nie, S. *Science* **1998**, *281*, 2016–2018.
- (8) Maxwell, D. J.; Taylor, J. R.; Nie, S. *J. Am. Chem. Soc.* **2002**, *124*, 9606–9612.
- (9) Cao, Y. C.; Jin, R.; Nam, J.-M.; Thaxton, C. S.; Mirkin, C. A. *J. Am. Chem. Soc.* **2003**, *125*, 14676–14677.
- (10) Soukka, T.; Harma, H.; Paukkunen, J.; Lovgren, T. *Anal. Chem.* **2001**, *73*, 2254–2260.
- (11) Wang, S.; Mamedova, N.; Kotov, N. A.; Chen, W.; Studer, J. *Nano Lett.* **2002**, *2*, 817–822.
- (12) Hirsch, L. R.; Jackson, J. B.; Lee, A.; Halas, N. J.; West, J. L. *Anal. Chem.* **2003**, *75*, 2377–2381.
- (13) Alivisatos, A. P.; Johnsson, K. P.; Peng, X.; Wilson, T. E.; Loweth, C. J.; Bruchez, M. P.; Schultz, P. G. *Nature* **1996**, *382*, 609–611.
- (14) Matsui, H.; Porrata, P.; Douberly, G. E. *J. Nano Lett.* **2001**, *1*, 461–464.
- (15) Ryadnov, M. G.; Ceyhan, B.; Niemeyer, C. M.; Woolfson, D. N. *J. Am. Chem. Soc.* **2003**, *125*, 9388–9394.
- (16) Li, H.; Park, S. H.; Reif, J. H.; LaBean, T. H.; Yan, H. *J. Am. Chem. Soc.* **2004**, *126*, 418–419.
- (17) Elghanian, R.; Storhoff, J. J.; Mucic, R. C.; Letsinger, R. L.; Mirkin, C. A. *Science* **1997**, *277*, 1078–1081.
- (18) Loweth, C. J.; Caldwell, W. B.; Peng, X. G.; Alivisatos, A. P.; Schultz, P. G. *Angew. Chem., Int. Ed. Engl.* **1999**, *38*, 1808–1812.
- (19) Zanchet, D.; Micheel, C. M.; Parak, W. J.; Gerion, D.; Alivisatos, A. P. *Nano Lett.* **2001**, *1*, 32–35.
- (20) Zanchet, D.; Micheel, C. M.; Parak, W. J.; Gerion, D.; Williams, S. C.; Alivisatos, A. P. *J. Phys. Chem. B* **2002**, *106*, 11758–11763.
- (21) Parak, W. J.; Pellegrino, T.; Micheel, C. M.; Gerion, D.; Williams, S. C.; Alivisatos, A. P. *Nano Lett.* **2003**, *3*, 33–36.
- (22) Mamedova, N. N.; Kotov, N. A.; Rogach, A. L.; Studer, J. *Nano Lett.* **2001**, *1*, 281–286.
- (23) Lebowitz, J.; Lewis, M. S.; Schuck, P. *Protein Sci.* **2002**, *11*, 2067–2079.
- (24) Murray, C. B.; Norris, D. J.; Bawendi, M. G. *J. Am. Chem. Soc.* **1993**, *115*, 8706–8715.
- (25) Gole, A.; Dash, C.; Ramakrishnan, V.; Sainkar, S. R.; Mandale, A. B.; Rao, M.; Sastry, M. *Langmuir* **2001**, *17*, 1674–1679.
- (26) Gole, A.; Dash, C.; Soman, C.; Sainkar, S. R.; Rao, M.; Sastry, M. *Bioconjugate Chem.* **2001**, *12*, 684–690.
- (27) Machtle, W. *Biophys. J.* **1999**, *76*, 1080–1091.
- (28) Dollefeld, H.; Hoppe, K.; Kolny, J.; Schilling, K.; Weller, H.; Eychmuller, A. *Phys. Chem. Chem. Phys.* **2002**, *19*, 4747–4753.
- (29) Colfen, H.; Tirosh, S.; Zaban, A. *Langmuir* **2003**, *19*, 10654–10659.
- (30) Mayya, K. S.; Schoeler, B.; Caruso, F. *Adv. Funct. Mater.* **2003**, *13*, 183–188.
- (31) Taylor, J. R.; Fang, M. M.; Nie, S. M. *Anal. Chem.* **2000**, *72*, 1979–1986.
- (32) Pena, S. R. N.; Raina, S.; Goodrich, G. P.; Fedoroff, N. V.; Keating, C. D. *J. Am. Chem. Soc.* **2002**, *124*, 7314–7323.
- (33) Yun, C. S.; Khitrov, G. A.; Vergona, D. E.; Reich, N. O.; Strouse, G. F. *J. Am. Chem. Soc.* **2002**, *124*, 7644–7645.
- (34) Keren, K.; Krueger, M.; Gilad, R.; Ben-Yoseph, G.; Sivan, U.; Braun, E. *Science* **2002**, *297*, 72–75.
- (35) Matthews, K. S.; Nichols, J. C. *Prog. Nucl. Acid Res. Mol. Biol.* **1998**, *58*, 127–164.
- (36) Frens, G. *Nature (London) Phys. Sci.* **1973**, *241*, 20.
- (37) Chen, J.; Matthews, K. S. *J. Biol. Chem.* **1992**, *267*, 13843–13850.
- (38) Wycuff, D. R.; Matthews, K. S. *Anal. Biochem.* **2000**, *277*, 67–73.
- (39) Demeler, B.; UltraScan 6.2 ed.; <http://www.ultrascan.uthscsa.edu/>, 2003.
- (40) van Holde, K. E.; Weischet, W. O. *Biopolymers* **1978**, *17*, 1387–1403.
- (41) Demeler, B.; Saber, H.; Hansen, J. C. *Biophys. J.* **1997**, *72*, 397–407.
- (42) Baudhuin, P.; Van der Smissen, P.; Beauvois, S.; Courtoy, P. J. In *Colloidal Gold: Principles, Methods and Applications*; Hayat, M. A., Ed.; Academic Press: San Diego, CA, 1989; Vol. 2, pp 2–18.
- (43) Lewis, M.; Chang, G.; Horton, N. C.; Kercher, M. A.; Pace, H. C.; Schumacher, M. A.; Brennan, R. G.; Lu, P. *Science* **1996**, *271*, 1247–1254.

NL047926F